

## THERMALLY ASSISTED EMISSION OF ELECTRONS AND VUV PHOTONS FROM IRRADIATED RARE GAS SOLIDS

E. V. SAVCHENKO, O. N. GRIGORASHCHENKO,  
A. N. OGURTSOV and V. V. RUDENKOV  
*Verkin Institute for Low Temperature Physics & Engineering NASU,  
Kharkov 61103, Ukraine*

G. B. GUMENCHUK  
*Institute of Radioastronomy NASU, Kharkov 61002, Ukraine*

M. LORENZ, A. M. SMITH-GICKLHORN, M. FRANKOWSKI\* and V. E. BONDYBEY  
*Institut für Physikalische und Theoretische Chemie der TU München,  
Garching 85747, Germany*

Relaxation processes and stability of charge centers in preirradiated doped rare gas solids were studied combining spectrally resolved thermally stimulated luminescence (TSL) and exoelectron emission (TSEE) techniques. The thermally assisted emission of electrons was found. Comparison of the yields of electrons and photons in VUV and visible ranges made it possible for the first time to discriminate between reactions of neutral species and charge carriers and find their interconnection. Ranges of charge center thermostability were found.

### 1. Introduction

Interaction of ionizing radiation with insulators turns them into metastable solids containing charge carriers, guest atoms, radicals and defect of structure. Energy absorbed during the irradiation and stored by these centers can be released by heating of samples triggering a complex series of reactions followed by energy conversion and transfer processes. Understanding thermally assisted physical and chemical processes in irradiated solids is of considerable interest both from the point of view of fundamental solid state physics, and a number of important applications in dosimetry, photochemistry, material and surface sciences.

Important information on energy relaxation, recombination and diffusion processes can be obtained by methods of thermally activated spectroscopy. Thermally stimulated luminescence (TSL)

is a valuable tool for studying recombination and relaxation paths in metastable solids as well as for trap-level analysis.<sup>1</sup> However, an interpretation of TSL data is complicated by the fact that it can stem both from charge carrier recombination and from thermally driven chemical reactions of neutral fragments.<sup>2,3</sup> To distinguish these processes the TSL method may be combined with measurements of thermally stimulated conductivity (TSC) or thermally stimulated emission of electrons (TSEE) from the sample into vacuum.

In this paper we present the results obtained combining the techniques of spectrally resolved TSL and TSEE applied to rare gas solids (RGS). These model insulators are the widest band gap solids in nature. An excitation above energy gap  $E_g$  results in electron-hole pair formation. Strong interaction with acoustic phonons causes hole self-trapping in

---

\*Permanent address: IF-FM Pol. Acad. Sci., Gdańsk, Poland

the lattice of all RGS. It was shown theoretically<sup>4</sup> as well as then experimentally<sup>5–7</sup> that the self-trapped holes (STH) have a configuration of molecular ionic dimers  $\text{Rg}_2^+$ . Those can be considered as intrinsic ionic centers in the lattice. The STHs are stable as long as electrons are trapped at defects of structure or guests with positive electron affinity. Self-trapping of electrons was found only in solid He and suggested in Ne.<sup>4</sup> In solid Ar, Kr and Xe the free conduction electron state is more stable than the localized one and electrons released from the traps by heating or by photons are highly mobile. Several studies of TSL from nominally pure RGS<sup>8–10</sup> and from doped ones<sup>11–15</sup> were reported. However, there are only a few experimental studies of intrinsic recombination VUV emission stimulated by heating<sup>7,8,12</sup> of RGS after exposure to ionizing radiation. This emission corresponds to luminescence of self-trapped excitons which can be viewed as  $\text{Rg}_2^*$  centers in the lattice. The techniques of thermally stimulated currents were rarely applied to RGS. To the best of our knowledge only two TSC studies of doped Ar and Kr solids were performed,<sup>13,16</sup> however, without TSL analysis in VUV.

## 2. Experimental Section

### 2.1. Sample preparation

Samples of RGS were grown from the gas phase by condensation on a cooled metal substrate. The structure of samples and therefore charge trap levels and their distribution within the energy gap were varied by changing deposition temperature and gas flow parameters — deposition mode (pulsed or continuous), flow speed, pulse duration and frequency. For the most part we used pulsed deposition. A typical deposition rate was kept at about  $10^{-2} \mu\text{ms}^{-1}$ . High-purity (99.999%) Ar gas was used. CO,  $\text{N}_2$  and  $\text{O}_2$  were used as dopants. Before the experiment, the gas-handling system was degassed by heating under pumping. The pressure in the deposition chamber was  $6 \cdot 10^{-8}$  mbar. The presence of impurities and dopants was monitored with a mass spectrometer and by the measurement of the infrared absorption spectrum. The mass spectrum of the residual gases showed lines of  $\text{N}_2$ ,  $\text{O}_2$ ,  $\text{H}_2\text{O}$ ,  $\text{CO}_2$ . The contamination was smaller than  $10^{-4}$ . The following characteristic impurity bands were used for the control:  $\text{H}_2\text{O} - 1631 \text{ cm}^{-1}$ ;  $\text{CO}_2 - 2338.7 \text{ cm}^{-1}$ ;

$\text{CO} - 2140.9 \text{ cm}^{-1}$ . The deposition rate and the sample thickness were determined by measuring the pressure decrease in a known volume and by observing fringes in the IR spectrum. A typical sample thickness was  $100 \mu\text{m}$ .

### 2.2. Charge center generation

To ionize the samples we used an electron beam because the ionization cross-section in this case is by a factor of  $10^2$  greater than that at photoionization. Charged centers were generated in two ways: (i) by irradiation of the grown neutral sample and (ii) by deposition of the gas under electron bombardment. In case (i) the thickness of the subsurface layer containing charged centers depends on the electron beam energy and can be easily varied. Using the (ii) way it was possible to generate charged centers across the whole sample. In both cases we used slow electrons of energy 120 eV (close to the maximum of ionization cross-section 50 eV) in case (ii) and up to 1 keV in case (i). The current density of the electron beam was kept at about  $0.1 \text{ mAcm}^{-2}$  in case (i) and  $0.03 \text{ mAcm}^{-2}$  at the deposition under the electron beam.

### 2.3. Activation spectroscopy

In our study a release of electrons from the traps and their transport were detected by measuring of TSEE as well as recording yields of recombination luminescence. In addition we detected photostimulated exoelectron emission (PSEE). Recombination of electrons with intrinsic ionic centers is followed by an emission of self-trapped excitons (so-called M-band). A range of recombination emission of positively charged guest centers depends on their level location within the band gap. Yields of visible and VUV light were detected with a conventional and solar-blind PMT. The total yield of TSL was measured with a PMT sensitized to VUV light. In addition we measured yields of spectrally resolved emissions at the wavelength of the intrinsic recombination luminescence and TSL of the dopant. The emission of electrons from preirradiated samples was detected with a movable Au-coated Faraday plate kept at a small positive potential (9 V). It was positioned at a distance of 5 mm in front of the sample grown on a grounded substrate. As the substrate we

used a silver-coated copper mirror, whose temperature was measured with a calibrated silicon diode sensor. A programmable temperature controller permitted us to keep the desired temperature and heating regimes. In most experiments we used a linear heating with the rate of  $3.2 \text{ Kmin}^{-1}$ . The current from the Faraday plate was amplified by a FEMTO DLPCA 100 current amplifier. The converted voltage was reversed in the polarity by an inverter and digitized in a PC. A current as low as 100 fA can be easily detected. In the PSEE experiments a Coherent 899-05 dye laser using Stilbene 3 and pumped with a Coherent argon ion laser (Innova 200) was used.

### 3. Results and Discussion

#### 3.1. TSL study

Because of the high ionization potentials  $I$  of the light RGS, Ne and Ar are the matrices of choice for studies of relaxation processes in these materials. We have first concentrated on the study of doped Ar solids in view of a wider temperature range available.  $I(\text{CO}) = 14.01 \text{ eV}$  and  $\text{CO}^+$  centers can be generated in Ar matrix due to high  $I$  of Ar ( $I = 15.759 \text{ eV}$ ). In solid Ar the band gap at the  $\Gamma$ -point is  $E_g = 14.16 \text{ eV}$ .<sup>17</sup> The other dopants were chosen to produce under irradiation transient species (N, O) capable of diffusing through the matrix under heating. Note that O atoms in their ground state  $^3\text{P}$  are effective deep traps for electrons because of the high electron affinity  $E_a = 1.46 \text{ eV}$ .<sup>18</sup>  $E_a$  of atomic N in the ground  $^4\text{S}$ -state is of  $-0.1 \text{ eV}$ <sup>19</sup> and these radicals cannot be seen as electron scavengers. The VUV luminescence of CO doped solid Ar under band-to-band excitation is shown in Fig. 1. It consists of known M-band stemming from the radiative decay of molecular centers  $\text{Ar}_2^*$  ( $1,3\Sigma_u^+ \rightarrow 1\Sigma_g^+$ ), wide band about 6.2 eV identified<sup>20</sup> as transition of self-trapped holes  $\text{Ar}_2^{+*}$  and Cameron bands ( $a^3\Pi \rightarrow X^1\Sigma^+$ ) of matrix isolated CO. The most intensive bands (0-0, 0-1, 0-2) of the progression are shown in Fig. 1. Note that the M-band and Cameron bands are effectively excited following primary creation of electron-hole pairs.<sup>21</sup> Sensitivity of the CO emission to the existence of electrons in the conduction band of solid  $\text{Ar}^{14}$  and high negative affinity  $E_a = -1.6 \text{ eV}$ <sup>22</sup> make it suitable for TSL studies along with the M-band. The total yield of TSL (curve c), yields of (0-1)

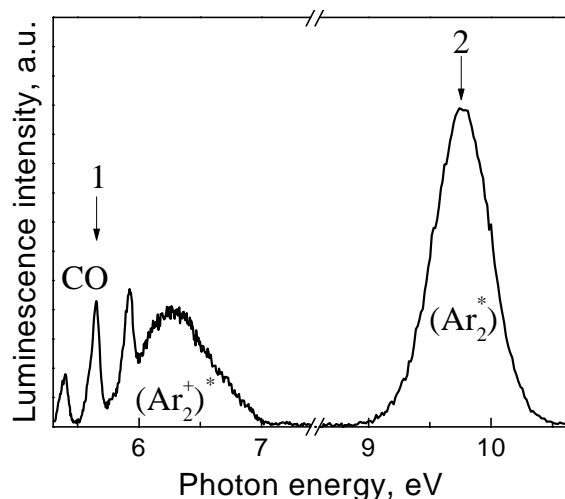


Fig. 1. Luminescence of CO-doped solid Ar, excited with  $h\nu = 14.2 \text{ eV}$  at 5 K.<sup>21</sup> Arrows indicate the photon energies used for spectrally resolved TSL measurements.

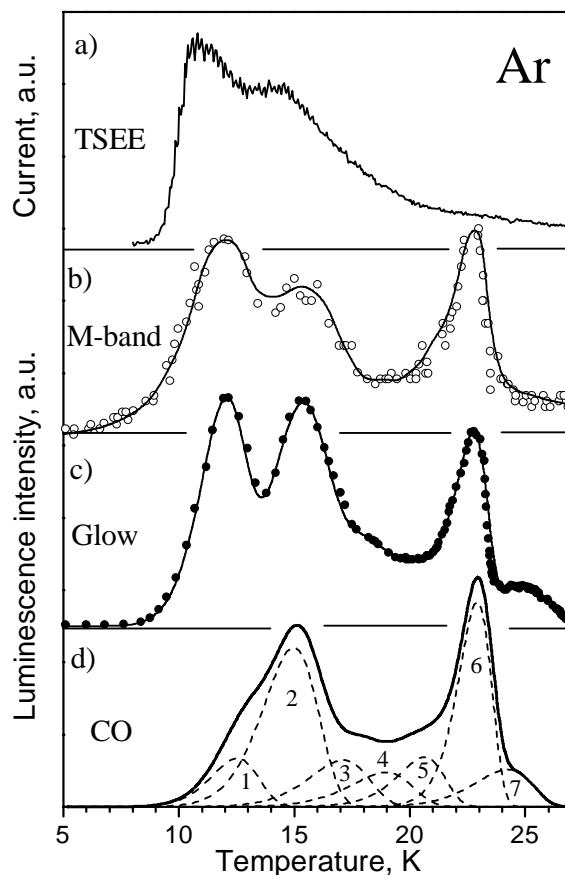


Fig. 2. Total yields of TSEE (a) and TSL (c). Spectrally resolved TSL (b, d) recorded at the photon energies shown in Fig. 1. Deconvolution of the CO TSL curve into first-order peaks is presented in the low curve.

the Cameron emission band (d) and the M-band (b) are shown in Fig. 2 along with the results of curve fitting assuming first-order kinetics.<sup>14</sup> The first low-temperature peak centered at 12 K is clearly seen in the total yield of the TSL (c) and in spectrally resolved intrinsic recombination luminescence (b). In the TSL at the wavelength of CO emission, the 12 K peak is fairly weak. Taking into account the low concentration of the dopant (0.1%) spread over the bulk of the sample, one can expect a low probability of  $\text{CO}^+$  recombination with electrons at the surface. This observation suggests that mainly surface traps contribute to this peak. The peak at 15 K was attributed to a formation of Frenkel pairs (vacancies and interstitials) based on the dose dependence of this peak.<sup>10</sup> A generation of point defects in solid Ar under irradiation by low-energy electrons was observed in Ref. 6. Both of these peaks are observed in a current curve — thermally stimulated exoelectron emission from solid Ar (curve a), which will be discussed in the next subsection. The peak around 22 K is observed in the total yield of the TSL, in the yields of intrinsic and extrinsic recombination luminescence. The peak was also detected in glow curve taken from nominally pure solid Ar irradiated by X-rays at 15 K<sup>9</sup> and by monitoring emission from  $\text{O}_2$ -doped Ar matrix (the Herzberg progression).<sup>13</sup> It was speculated there that this peak in TSL is caused by chemiluminescence accompanied by the recombination of  $\text{O}^-$  ions with neutral O atoms. To clarify an origin of this peak we turn our attention to the behavior of thermally stimulated currents.

### 3.2. TSEE study

The TSEE yield from nominally pure Ar is shown in Fig. 2 (curve a) and from Ar matrices doped with  $\text{N}_2$  (a) and CO (b) in Fig. 3. The structure of current curves depends on crystal quality, the kind and content of the dopant, residual gas contamination and the prehistory of the sample. However, samples grown in an identical way exhibited quite reproducible TSEE curves. Two peaks at 12 K and 15 K are characteristic of all Ar solids. Their identification was discussed in the previous subsection. Doping with 0.1%  $\text{O}_2$  (not shown in the figure) resulted in a strong suppression of TSEE from samples because of an increase in the concentration of deep traps. Note that  $\text{O}_2$  centers are also effective traps of electrons

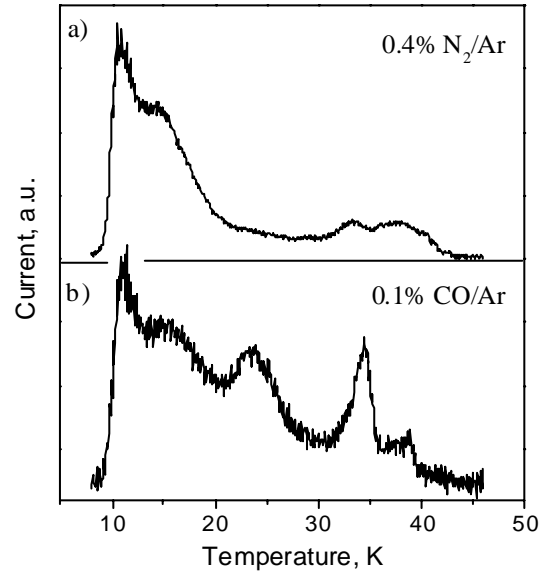
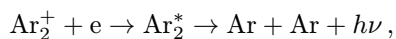


Fig. 3. TSEE current curves measured from solid Ar doped with 0.4%  $\text{N}_2$  (curve a) and 0.1% CO (curve b).

( $E_a = 0.44$  eV<sup>23</sup>). The presence of small contents (0.01%) of  $\text{O}_2$  resulted in an emergence of the peak at 22 K. Doping with  $\text{N}_2$  caused an enhancement of high-temperature peaks above 30 K. In nitrogen-containing samples a long-lived afterglow and “afteremission” were observed due to the well-known long lifetime transition  $^2\text{D} \rightarrow ^4\text{S}$  of N atoms with characteristic decay time  $\tau$  of about 20 s.<sup>24</sup> Note that the  $\tau$  of exponential decay extracted from the current curves of the “afteremission” depends on the sample structure.

The TSEE curve with well-defined peaks was measured from a CO-doped sample which was annealed at 23 K and then photolyzed before the irradiation at  $T = 8$  K. The sample contained O and N atoms. The TSEE yield was taken after the decay of the “afteremission.” A content of neutral CO in the matrix monitored by absorption measurement increased during the heating. There is a good reason to believe that the peak at 22 K in the TSEE yield stems from thermally stimulated recombination of O atoms. The subsequent cycle of irradiation (without photolysis) and heating showed no distinctive feature at  $T = 22$  K. The peak around 30 K demonstrates a similar behavior. The interpretation of high-temperature peaks is hampered because the TSEE curves are affected by a sublimation of sample at  $T > 30$  K.

The current curves give direct evidence of the appearance of mobile negatively charged carriers (more likely electrons) upon heating of the preirradiated samples. A correlation between TSEE and TSL peaks indicates common relaxation processes underlying these phenomena. Electrons released from traps by heating and promoted to the conduction band can then escape from the sample or reach positively charged centers and recombine yielding TSL by the reactions:



The whole set of data on the 22 K peak behavior — observation of the peak in spectrally resolved TSL yield in the intrinsic recombination emission (the M-band) and in the extrinsic one (Cameron bands) as well as in TSEE yield can be explained if one suggests the following scenario. In freeing and mobilizing electrons the energy could be transferred nonradiatively but more likely by the light emitted due to O radical recombination. An emission of the Herzberg bands was observed at  $T = 22 \text{ K}$ <sup>13</sup> along with TSC through the Ar matrix.

### 3.3. PSEE study

To verify the suggested scenario, a special experiment on photon-stimulated exoelectron emission was performed. The emission of electrons measured immediately after sample preparation — “afteremission” was measured (low curve in Fig. 4). On completion of its decay laser light was focused at the sample whilst the PSEE current was monitored as a function of time (upper curve in Fig. 4). The energy chosen for the excitation coincides with one of the Herzberg progression band. An intensive emission of electrons was found under laser excitation. Note that the current was observed at low temperature, which is out of the range of the TSEE. Test experiments have shown that no current is observed from the substrate and from nonirradiated sample of solid Ar as one can expect. The energy of photons used in the PSEE experiments was lower than the threshold energy of photoemission from the substrate (work function of Ag is of 4.74 eV). Kinetics of the PSEE current decay is described by a double exponential law with  $\tau_1 = 21 \text{ s}$  and  $\tau_2 = 190 \text{ s}$ . The long time

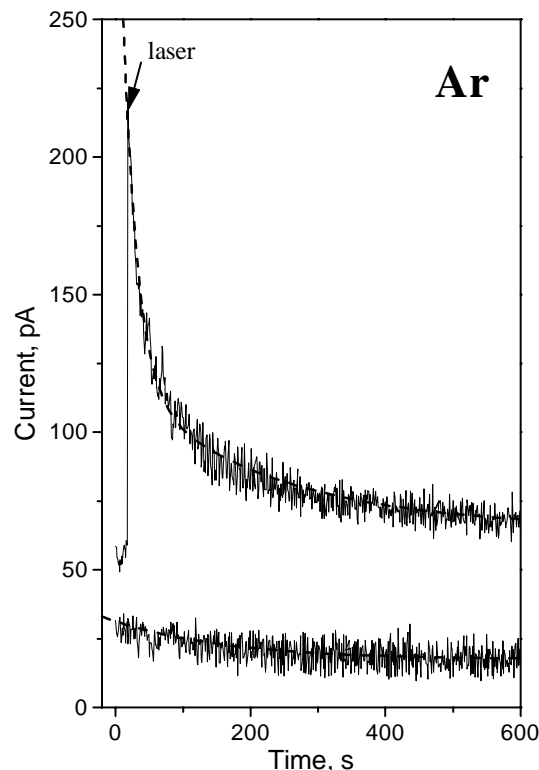


Fig. 4. Temporal variation of PSEE current from preirradiated solid Ar excited by laser light with  $h\nu = 2.76 \text{ eV}$  at  $T = 8 \text{ K}$ . The low curve shows “afteremission” observed from the sample.

coincides within the accuracy of fitting (30%) with the characteristic decay time of “afteremission” for this sample. PSEE is in fact the optical equivalent of TSEE. Photons whose energy is sufficient to excite the trapped electrons into the conduction band generate mobile electrons capable of escaping the solid. The decay of the free-carrier density  $N_c$  can be represented for the case of no-retrapping by a simple exponential expression,<sup>25</sup> which is

$$N_c = g\tau_c N_{t0} \exp(-gt),$$

where  $g$  is the product of the density of photons irradiating the sample and effective interaction cross-section of the photons and the electrons in the traps, and  $\tau_c$  is the effective lifetime of the electrons in the conduction band. For insulators containing space charge  $\tau_c$  is a complex function of the mobility of charge carriers, the applied voltage, the electrode spacing and its evaluation requires special experiments. The decaying portion of the current-time transient curve describes the decrease in mobile

electron density during trap emptying and  $\tau = g^{-1}$  estimated from the curve ( $\tau_1$  and  $\tau_2$ ) characterizes the effective interaction cross-section of the photons and electrons in definite kinds of traps. The fact that the PSEE curve is best fitted by the double exponent law associates with contributions of two kinds of traps with different parameters. One can expect a presence of deep traps  $O^-$  and  $O_2^-$ . Their binding energies are  $E_b(O^-) = 2.61$  eV and  $E_b(O_2^-) = 1.6$  eV.  $E_b$  were estimated by  $E_a$  corrected by polarization energy of Ar ( $-1.15$  eV).<sup>26</sup> The data obtained support the suggested mechanism of the conversion of chemical reaction energy into kinetic energy of electrons followed by charge transfer.

#### 4. Summary

Electronic processes of relaxation in preirradiated solid Ar doped with CO, N<sub>2</sub>, O<sub>2</sub> were studied by activation spectroscopy methods — TSL, TSEE and PSEE. Correlation of photon yields in VUV and visible ranges with electron yield enables one to discriminate between reactions of neutral and charged species, find their interconnection and reconstruct the cascade of energy and charge relaxation.

#### Acknowledgments

The authors thank Profs. G. Zimmerer and D. Menzel for valuable discussions. E. V. S. acknowledges BMBF.

#### References

1. *Luminescence of Solids*, ed. D. R. Vij (Plenum, New York, 1998).
2. V. E. Bondybey, M. Räsänen and A. Lammers, *Annu. Rep. Prog. Chem.* **C95**, 331 (1999).
3. V. A. Apkarian and N. Schwentner, *Chem. Rev.* **99**, 1481 (1999).
4. K. S. Song and R. T. Williams, *Self-Trapped Excitons*, Springer Series in Solid State Science, Vol. 105 (Springer-Verlag, Berlin, 1996).
5. E. V. Savchenko, N. Caspary, A. Lammers and V. E. Bondybey, *J. Low Temp. Phys.* **111**, 693 (1998).
6. E. V. Savchenko, A. N. Ogurtsov, O. N. Grigorashchenko and S. A. Gubin, *Low Temp. Phys.* **22**, 926 (1996).
7. E. V. Savchenko, O. N. Grigorashchenko, O. M. Sokolov, J. Agreiter, N. Caspary, A. Lammers and V. E. Bondybey, *J. Electron Spectrosc. Relat. Phenom.* **101–103**, 377 (1999).
8. M. Kirm and H. Niedrais, *J. Luminesc.* **60–61**, 611 (1994).
9. M. Kink, R. Kink, V. Kisand, J. Maksimov and M. Selg, *Nucl. Instrum. Methods* **B122**, 668 (1997).
10. A. N. Ogurtsov, E. V. Savchenko, O. N. Grigorashchenko, S. A. Gubin and I. Ya. Fugol', *Low Temp. Phys.* **22**, 922 (1996).
11. M. E. Fajardo and V. A. Apkarian, *J. Chem. Phys.* **89**, 4124 (1988).
12. A. V. Danilychev and V. A. Apkarian, *J. Chem. Phys.* **99**, 8617 (1993).
13. A. Schrimpf, C. Boekstiegel, H.-J. Stöckmann, T. Bornemann, K. Ibbeken, J. Kraft and B. Herkert, *J. Phys.: Condens. Matter* **8**, 3677 (1996).
14. J. Becker, O. N. Grigorashchenko, A. N. Ogurtsov, M. Runne, E. V. Savchenko and G. Zimmerer, *J. Phys. D: Appl. Phys.* **31**, 749 (1998).
15. L. K. Khriachtchev, M. Pettersson, S. Pehkonen, E. Isoniemi and M. Rasanen, *J. Chem. Phys.* **11**, 1650 (1999).
16. R. Dersch, B. Herkert, M. Witt, H.-J. Stockmann and H. Ackermann, *Z. Phys. B: Condens. Matter* **80**, 39 (1990).
17. G. Zimmerer, *Creation, Motion and Decay of Excitons in Rare-Gas Solids*, Excited-State Spectroscopy in Solids (Holland Pub. Co., Amsterdam, 1987), p. 37.
18. H. Hotop and W. C. Linberger, *J. Phys. Chem. Ref. Data* **14**, 731 (1985).
19. L. D. Thomas and R. K. Nesbet, *Phys. Rev.* **12**, 2369 (1975).
20. A. N. Ogurtsov, E. V. Savchenko, J. Becker, M. Runne and G. Zimmerer, *J. Luminesc.* **76–77**, 478 (1998).
21. A. N. Ogurtsov, E. V. Savchenko, J. Becker, M. Runne and G. Zimmerer, *Chem. Phys. Lett.* **281**, 281 (1997).
22. J. Balamuta and M. F. Golde, *J. Chem. Phys.* **76**, 2430 (1982).
23. R. C. Weast, *Handbook of Chemistry and Physics* (CRC, Florida, 1988).
24. R. E. Boltnev, E. B. Gordon, V. V. Khmelenko, I. N. Krushinskaya, M. V. Martynenko, A. A. Pelmenev, E. A. Popov and A. F. Shestakov, *Chem. Phys.* **189**, 367 (1994).
25. J. D. Brodribb, D. O'Colmain and D. M. Hughes, *J. Phys.* **D8**, 856 (1975).
26. L. E. Lyons and M. G. Sceats, *Chem. Phys. Lett.* **6**, 217 (1970).